Mausam, (1991), **42**, 2, 187-194

551.579.2

Use of satellite based information in snowmelt run-off studies

D. S. UPADHYAY, D. K. MISHRA, A. P. JOHRI, D. K. MISRA and A. K. SRIVASTAVA

Meteorological Office, New Delhi

(*Received 4 January 1988*)

सार — इस शोध-पत्र का उद्देश्य हिमतहों के पिघलने से बेसिन में प्राप्त जल राशि के अभिकलन के लिए एक वैचारिक तकनीक विकसित करना है। यह विशेष तौर से ग्रीष्म ऋतु के शुष्क समय में हिमगलन जनित अपवाह के आकलन में उपयोगी हो सकता है। इस के लिए मौसम उपग्रह NOAA-9 से प्राप्त अति उच्च वियोजन बिम्बावली के प्रयोग द्वारा सतलुज नदी के जल ग्रहण क्षेत्र में हिमतहों का माप कुछ चुनी हुई अवधि, (*i*) अक्तूबर 1985 से मई 1986, तथा (*ii*) जनवरी से जून 1987 के दौरान किया गया। गलन से प्राप्त अभिकलित जल की तुलना उपलब्ध वास्तविक अपवाह के आंकड़ों से की गई है।

अध्ययन ने यह दर्शाया है कि उपग्रह से प्राप्त हिम तहों के आंकड़े, हिमगलन अपवाह की प्रागुक्ति के लिए बहुत उपयोगी है। हिमालय के बृहत् जल संभरों के लिए जहां कि भूमि पर आधारित माप अत्यंत कम है इस तकनीक का महत्व और भी अधिक है।

ABSTRACT. This paper aims at evolving a conceptual technique for the computation of water yield from the basin snow cover. It may serve as a useful information to compute the snowmelt driven run-off particularly in the lean summer season. For this purpose, the measurement of snow cover area in catchment of *Satluj* river, using very high resolution imagery received from the meteorological satellite NOAA-9 was undertaken on selected dates during the periods, (*i*) October 1985 to May 1986, and (*ii*) January to June 1987. The computed snowmelt water yield have been compared with the available actual run-off data.

The study shows that the satellite derived snow cover data are potentially useful in predicting the snowmelt run-off. The importance of this technique is further enhanced for the large watersheds over Himalayas where ground based measurements are too scanty.

Key words —AVHRR, energy budget, glaciers, NOAA-9, run-off, snowmelt.

1. Introduction

Twenty two major Indian rivers originate from Himalayas which are primarily fed by snow and glaciers. There are about 5000 glaciers in their upper catchments covering an area over 33,000 km². During high winters area covered by seasonal snow is 30 to 50 times more than this.

This study aims at evolving a conceptual technique for the computation of water yield from the basin snow cover. Snowbound area of the catchment has been evaluated from satellite (NOAA-9) imageries by using zoom transfer scope. The technique has been illustrated for Satluj basin.

River *Satluj* rises from lake Rakas (4541 m; adjacent to Mansarovar) in Tibet. After completing a long course through mountain ranges of Himachal Pradesh, it emerges from Sivalik hills at Bhakra gorge and then widens into an alluvial river. Its total length from origin to Indo-Pak border is about 1070 km. Its major tributary Spiti joins at Khab (HP). The catchment of Satluj above Bhakra Dam covers an area of 57,244 km² of which only 22,310 km² lies in India. The altitude-wise distribution of Indian area up to Bhakra is given below :

Altitude range (*m*)	*Area* (*km²*)
0 - 1000	2610
1000 - 2000	2920
2000 - 3000	2280
3000 - 4000	2500
4000 - 5000	6480
5000 - 6000	5120
6000 - 7000	400
Total	22,310

The area of Satluj catchment over Tibet is a high land zone, where precipitation is very little and temperature is too low. Hence, the quantity of snowmelt is expected to be too low to contribute any significant water to river run-off.

2. Snow cover water storage

To estimate quantity of water stored in the form of snow cover we need three inputs : (*i*) areal extent of snow cover (*A*), (*ii*) mean density of snowpack (ρ), and (*iii*) mean depths of standing snow (*h*).

$$W = A.\rho.h$$

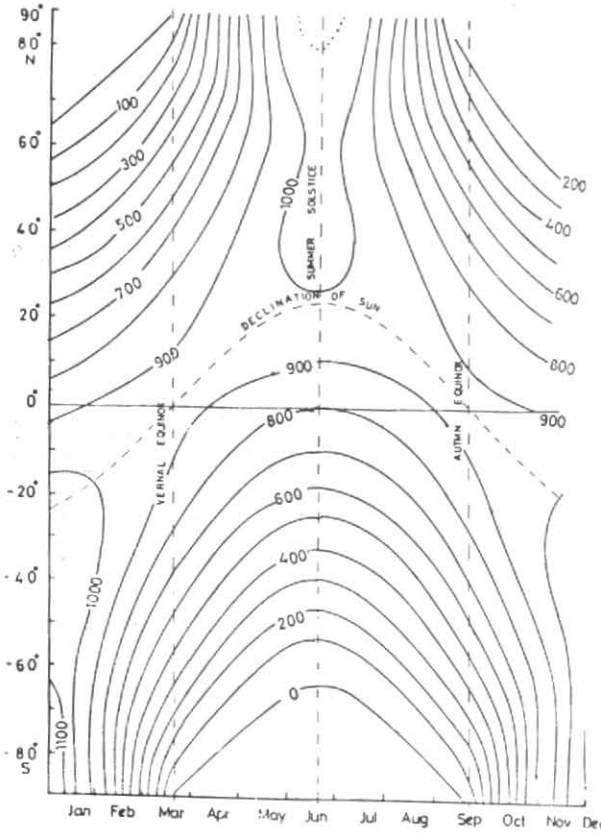

Fig. 1. Distribution of solar radiation at the top of atmosphere

Fig. 2. Map of catchment area of Satluj river showing snow cover on 10 February 1986

2.1. *Areal extent of snow cover*

It is generally expressed as percentage of the catchment area covered by snow. It depends on meteorological and topographical factors which control deposition or ablation of snow. A seasonal snow cover may be continuous or sporadic (in patches).Theoretically a snow line separates continuous snow cover from the snow free area. But in between the two areas, there lies perforated and sporadic snow patches. A snow line is then drawn along 50% coverage.

Areal snow cover extent over a small watershed can be estimated by snow mapping on the basis of ground observations of snow deposition, snow types (old snow, new snow, firn, hoar etc) snow state (hard, soft, dry, wet etc) and special formations (like cornices, drift deposits, avalanche deposits). After drawing snow line, the area may be delineated using a contour map of the basin. Photogrammetric pictures from aircraft (flying 1 to 3 km above ground) are also widely used for snow mapping.

However, the above techniques have limitations for long basins like Satluj. In such cases satellite pictures are useful tool for snow survey on cloud free days. We have used NOAA pictures for estimating areal extent of snow cover in Satluj for some days during 1985, 1986 and 1987. The procedure followed is given in section 4.

2.2. *Density of snow*

A snow crystal consists of ice, air and water; ice forming a frame work with air and water filling up the voids. A snow cover is a sheet of such crystals randomly arranged. The density of a snow cover depends on the void-ratio or porosity of the crystal.

Fresh or new snow has low density (<100 kg m^{-3}) and varies slightly with the temperature of ambient air (increases with rise of temperature). A snowpack is normally formed due to snow deposition in a number of spells. As such it consists of various layers of different texture. Mean density of snow cover is the weighted average of the densities of various layers using depths of these layers as the weights. During March-April when snow cover becomes ripe to yield meltwater, it assumes a uniform density of the order of 500 - 600 kg m^{-3}.

3. Snowmelt processes

These are basically two approach adopted for the computation of snowmelt, (*i*) degree day factor of empirical formula based on antecedent temperature conditions, and (*ii*) energy budget equation.

In this paper the second approach has been followed for which an outline is provided below :

Energy balance equation is :

$$Q = Q_{rs} + Q_{rl} + Q_c + Q_e + Q_g + Q_r \qquad (1)$$

where, Q_{rs} = Shortwave radiation input,

Q_{rl} = Longwave radiation input,

Q_c = Energy transfer due to conduction,

Q_e = Latent heat of condensation,

Q_g = Heat input to the snowpack from the ground underneath,

Q_r = Heat content of rainwater falling over the snow.

Q_g and Q_r are generally negligible as compared to the other components, hence we omit them in the present discussion. The positive sign is assigned to a value if it is a gain of energy to the snowpack and negative if energy is lost from the pack.

3.1. *Estimation of* Q_{rs}

Daily flux of Q_{rs} over a horizontal surface at the top of the atmosphere (R_o) depends on latitude of the place and time of the year. For practical use the values of R_o are presented in Fig. 1 for various latitudes and months. On a cloudless day the incident radiation on a snow surface may be given as (*Ref.* US Corps of Engrs. 1956).

$R = 0.80\ R_0$, during winter and

$R = 0.85\ R_0$, during summer.

It has been presumed that during winter the atmospheric transparency is slightly low due to difference in optical air masses. But in cases when the lower atmosphere has more dust content during summer the coefficient of transparency may be higher during winter months.

If N is the amount of cloudiness, the net radiation incident on the snow surface may be given as :

$$R_e = [\,1 - (0.82 - .000073\ Z)\ N\,]\ R \qquad (2)$$

where, N is in decimal fraction and Z = Cloud height in metres. If r is the albedo of snow surface,

$$Q_{rs} = (1 - r)\ R_e \qquad (3)$$

r is generally a function of, (a) age of the snow surface, and (b) water contents of the pack.

For practical purposes the following experimental values of albedo may be adopted (*Source*, Corps of Engrs., U. S. Army 1956).

Age of snow	*Accumulation period*	*Melt period*
(*Days*)	(*Dec-Feb*)	(*Mar-May*)
0	85	78
2	77	65
4	72	57
6	68	53
8	66	50
10	65	48
12	64	46
14	63	44

The radiation absorbed at snow surface penetrates the pack only to a few centimetres.

3.2. *Estimation of* Q_{rl}

In mountain regions, snow cover receives longwave radiation from, (a) atmospheric molecules like air, vapour, carbon dioxide, dust etc, (b) clouds, and (c) forest cover.

Considering emission from snow surafce as a black body radiation (emissivity=1) the intensity of longwave radiation input is:

$$I_n = \sigma\,(\,0.757\ T_a^4 - T_s^4) \qquad (4)$$

where, $\sigma = 0.826 \times 10^{-10}$ ly/min/deg^4,

The presence of clouds reduces the longwave radiation loss from snowpack. If N is the cloudiness, the net longwave radiation exchange over snowpack will be

$$Q_{rl} = I_n\,(1 - KN) \qquad (5)$$

where, the constant K depends on height of the clouds. As suggested by U.S. Corps. of Engrs 1956, for:

Low and thick clouds; $K = 0.76$

Medium clouds; $K = 0.52$

High clouds; $K = 0.26$

3.3. *Estimation of* Q_c *and* Q_e

Using well known equations of turbulent exchange of any property such as specific humidity (q) or temperature (T) the expressions for Q_e and Q_c have been derived by various authors. One such expression is :

$$Q_e = 5.487\,(e_a - e_s)\ U$$
$$\text{and}\quad Q_c = 0.527\ \ (T_a - T_s)\ U \qquad (6)$$

where, e_a (mb) is the vapour pressure at screen level, air temp. T_a (°C), e_s (mb) is s.v.p. at snow surface temperature T_s. U is the wind speed (mph) recorded at 16 feet above ground level.

3.4. *Estimation of* Q_g

Due to poor thermal conductivity of the soil and snow condution of heat from the ground underneath is comparatively negligible (of the order of 1 to 5 ly/day).

3.5. *Estimation of* Q_r

When rainfall occurs over seasonal snow cover, it releases its heat content and accelerates the rate of melting. During spring months the entire snowpack is isothermal around 0°C. If r cm of rainfalls over snow, it releases $r\,(T_w - T_s)$ calories of heat, where T_w and T_s are the wet bulb and snow surface temperature (°C) respectively.

Considering $\quad T_s = 0°C,$

$\qquad\qquad Q_r = r\,T_w.$

4. Snow mapping from satellite imagery

The authors have used pictures taken by the Advance Very High Resolution Radiometer (AVHRR) sensor on board the U. S. polar orbiting satellites of NOAA series for measuring the snow cover area of catchment of river *Satluj* (west of longitude 78.6°E). Whatever run-off due to snowmelt comes from Satluj catchment lying east of 78.6°E, has been accounted for by the actual run-off measurement at Namgia and Rampur. The AVHRR

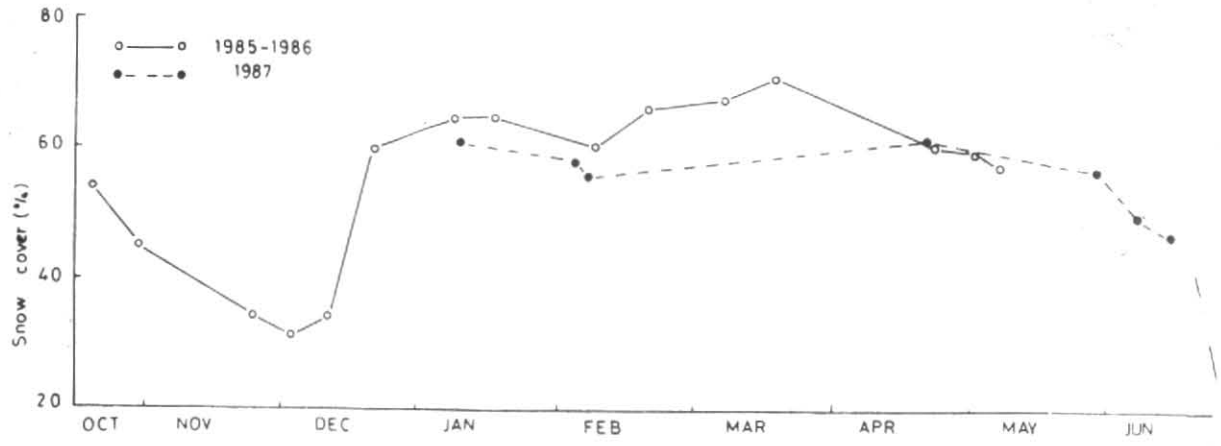

Fig. 3. Percentage snow cover over Satluj catchment 1985-1986 and 1987

TABLE 1

Satellite derived snow cover area

Date	Area under snow cover Satluj Basin (Indian part) (km^2)	% area under snow	Altitude of of snow line (m)	Freezing level (m)	Incident Radiation R_e (ly/day)	Albedo fraction (r)
			1985			
18 Oct	12075	54	2987	3750	442	.70
28 Oct	10010	45	3814	3750	338	.70
23 Nov	7665	34	4290	3300	388	.65
02 Dec	7000	31	4393	2550	347	.60
10 Dec	7735	35	4279	2550	347	.60
19 Dec	13509	61	2358	2550	206	.60
			1986			
07 Jan	14392	64	1977	2000	243	.75
15 Jan	14392	64	1977	2200	354	.75
07 Feb	13377	60	2416	2425	435	.75
19 Feb	14770	66	1848	2425	401	.75
05 Mar	15120	68	1728	3100	473	.60
16 Mar	15750	71	1512	3100	435	.60
21 Apr	13475	60	2373	3800	523	.50
30 Apr	13321	60	2411	3800	523	.50
05 May	12831	57	2856	4250	595	.40
			1987			
08 Jan	13720	61	2266	2000	354	.75
04 Feb	13062	58	2554	2425	410	.75
07 Feb	12389	55	2850	2425	394	.75
20 Apr	13649	61	2297	3800	438	.50
27 May	12880	57	2634	4250	474	.40
06 Jun	10920	49	3450	4750	694	.35
13 Jun	10570	47	3590	4750	694	.35

sensor provides imagery at a ground resolution of 1.1 km in 5 spectral channels. Satellite pictures received in visible (0.55 - 0.9 μm waveband) and thermal infrared (10.5-11.5 μm) channels have been utilized in this study. Both visible and infrared pictures have been used to remove cloud contaminated snow cover pictures and to select only the cloud-free pictures for snow cover analysis. The map of snow cover area is produced by enlarging and rectifying the visible channel picture in order to match with the river basin map. The registration of the satellite picture with the map involved coinciding the physiographic landmarks (*e. g.*, lakes, rivers and ridges) using the optical registration device called zoom transfer scope. The rivers on the drainage map are then aligned with the respective rivers valleys identified in the AVHRR picture. The snow cover map is then traced on the river catchment map and measured manually with a planimeter. This simple technique gives satisfactory results, although more advanced computer based systems can be used for image registration and area measurement. The variations in the area of snow cover in Satluj basin have thus been measured and their relationship with the resulting run-off studied.

A map of catchment showing snow cover on 10 February 1986 is shown at Fig. 2. The percentage snow cover over Satluj catchment on various dates have been presented graphically in Fig. 3 (1985-1986 and 1987) and given in Table 1.

5. Determination of freezing level and snowline

The maximum contribution of snowmelt occurs from the snow cover lying between snowline and the freezing level. For determining the altitude of freezing level, the temperature analysis of various stations situated at different altitude has been carried out.These stations are Mandi (761 m), Bhuntar (1067 m), Dharamsala (1211 m), Manali (2039 m), Shimla (2202 m) and Leh (3514 m). From this study, Fig. 4 and Fig. 5 have been worked out which provide mean lapse rate of surface temperature during different months. Freezing levels have been estimated from the point of intersection of these lines with y-axis. The area between snowlin and freezing level has been taken as the contributing snowpack to the meltwater yields (Table 2).

6. The computation of energy budget and snowmelt

(a) *Short-wave solar radiation* (Q_{rs})

The radiation values R_o reaching at the top of atmosphere in different months have been adopted from standard tables. Applying the transparency correction given in section 4 and the adjustment for cloudiness N, the radiation reaching at snow surface worked out as:

$$R = R_o \ [.3 + .5 \ (1 - N)]$$

(b) Longwave radiation input available for snowmelt has been computed using relations (4) and (5). The air temperature was estimated for the level midway between snowline and freezing level. If this level is named as meltlevel (M_L) then :

$$M_L = \frac{S_L + F_L}{2}$$

using the temperatures recorded at Shimla (2202 m), the following mean lapse rates [(L_R) in °C/km] derived from Figs. 4 and 5 were applied :

Month	O	N	D	J	F	M	A	M	J
L_R (°C/km)	6.9	7.2	8.6	11.0	10.0	9.1	8.0	8.0	8.0

The computed values of T_a have been given in Appendix. T_s has been estimated from the empirical results used by Upadhyay (1981).

(c) Q_c *and* Q_e

The values of Q_c and Q_e have been calculated using met data of Shimla and interpolating them to the mean altitude of snow cover. The equations discussed in section 3 have been applied.

(d) *Computation of snowmelt*

If Q is the energy input to the snowpack, the depth of snowmelt (M) is given by $M = Q/80$, assuming that the thermal quality of snow is unity. This depth multiplied by the snow cover area between snowline and freezing level provides the volume of meltwater.

7. Discussion, results and limitations

Presuming that the snow cover lying below the altitude of freezing level mainly contributes to the water yield, the area of snow between snowline and freezing level has been linearly interpolated from the area elevation relationship. This area multiplied by the depth of snowmelt gives the volume of meltwater. The meltwater in the unit of cumec are given in columns 9 and 10 of Table 2. The following inferences are apparent:

(*i*) During high winter, there is no significant meltwater available. This may be either due to negative heat input to the snow or due to freezing level being lower than the snowline. This is clearly reflected in discharge observations recorded at Bhakra which shows the minimum flow (base flow) during the high winter (of the order of 100 cumec).

(*ii*) From March onwards, the heat input becomes significant and melt rate increases gradually. Freezing level rises faster than the snowline. It also increases the snow cover area between F_L and S_L. But one has to remember that this area is slopy and the snow cover resting on it will be highly sporadic in nature.

Also the satellite imageries used here have a resolution of 1.1 km. It is possible that the sporadic nature of snow cover which is a common feature during the hot weather months remains unnoticed in satellite data. To make up for this deficiency in observation, it is proposed to take a factor of 0.5 arbitrarily representing a ratio of snow cover between snowline and freezing level from March to June.

(*iii*) The volume of meltwater becomes very high during March and onwards, as seen from column 10. The rate of increase is not reflected in discharge observations which show a rather slower increase. This may be attributed to the following two reasons:

(a) The snow is not fully ripe before June. Till then, much of meltwater percolates through the cover and fills up the pores of the snowpack.

(b) A large quantity of meltwater is also lost in evaporation, infiltration and retention in surface depressions.

(*iv*) Some indicative inferences showing of meltwater contribution to river run-off is provided in Table 3.

During winter months, the snowmelt is very little and practically no contribution occurs to river run-off. Although, the meltwater is less during October November but most of it goes to river because loss factor seems to be negligible.

(*v*) The rate of snowmelt increases from March to June/July and the snow cover area increases during this

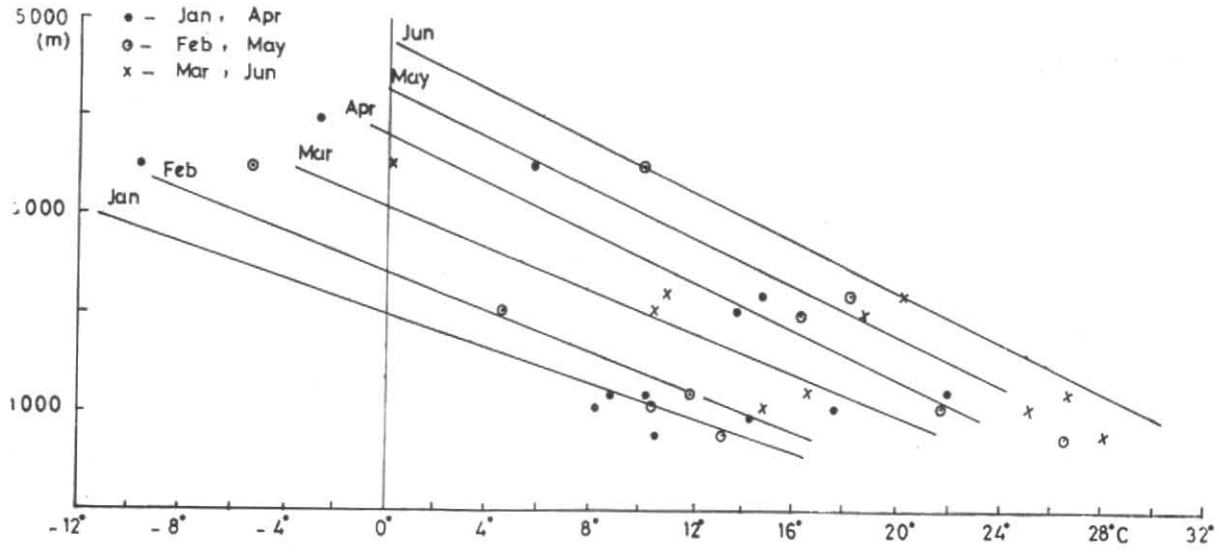

Fig. 4. Lapse rate of surface temperature

TABLE 2

Snowmelt computations

Date	Q_{rs} (ly/day)	Q_{rl} (ly/day)	Q_e (ly/day)	Q_c (ly/day)	Q (ly/day)	$M=Q/80$ (cm)	Area (km²) between F_L & S_L	Water yield (Cumec)	Discharge at Bhakra (Cumec)
(1)	(2)	(3)	(4)	(5)	(6)	(7)	(8)	(9)	10)
				1985					
18 Oct	133	—131	19	4	25	0.3	1905	66.1	332
23 Nov	136	—163	—3	—1	—31	—0.4	—	—	138
02 Dec	139	—165	—1	0	—27	—0.3	—	—	113
10 Dec	139	—161	—4	—1	—27	—0.3	—	—	150
19 Dec	122	—114	6	1	16	0.2	438	10.1	140
				1986					
07 Jan	61	—64	100	14	110	1.4	67	10.9	135
15 Jan	89	—100	58	10	57	0.7	67	5.4	125
07 Feb	109	—116	31	5	28	0.4	21	1.0	94
19 Feb	100	—108	25	5	22	0.3	1413	49.1	104
05 Mar	189	—92	34	5	136	1.7	3324	327.0	133
16 Mar	174	—105	33	6	108	1.4	3955	320.5	161
21 Apr	261	—57	56	8	268	3.4	3430	674.9	225
30 Apr	261	—92	34	5	208	2.6	3275	492.8	250
05 May	357	—100	58	10	325	4.1	4904	1163.6	247
				1987					
08 Jan	89	—92	17	3	17	0.2	—	—	N.A.
04 Feb	103	—139	14	3	—19	—0.2	—	—	N.A.
07 Feb	99	—122	25	5	7	0.1	—	—	N.A.
20 Apr	219	—57	25	4	191	2.4	3603	500.4	N.A.
27 May	284	—81	20	3	226	2.8	4954	802.7	N.A.
06 Jun	451	—108	0	0	343	4.3	5263	1309.7	N.A.
13 Jun	451	—131	6	1	327	4.1	4888	1159.8	N.A.

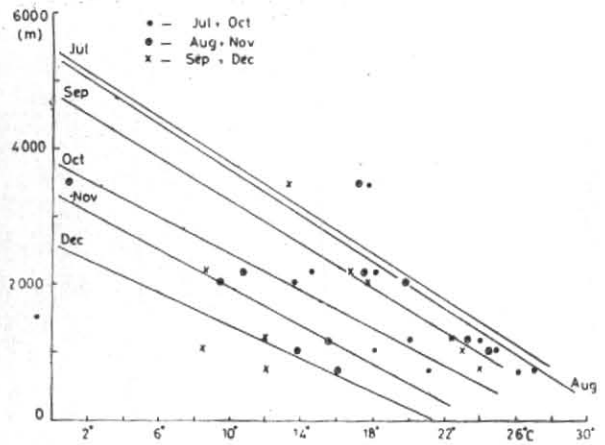

Fig. 5. Lapse rate of surface temperature

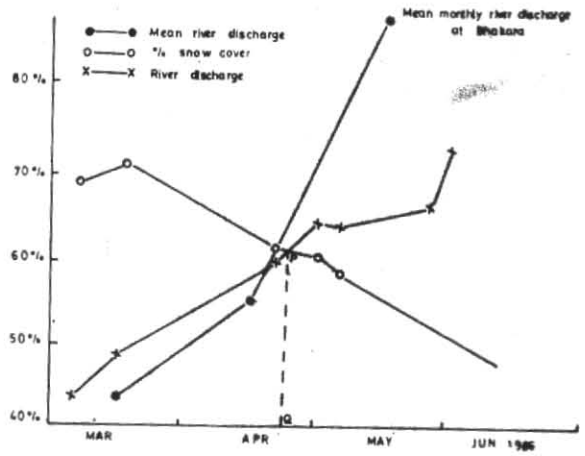

Fig. 6. Percentage snow cover river *Satluj* catchment and net discharge at Bhakra.

TABLE 3

Month	Snow cover area (km^2)	Snow cover area contributing to melt (km^2)	Melt water (Cumec)	% of melt water which may contribute river flow
Jan	14000	Nil	Nil	Nil
Feb	13000	500	14.3	Nil
Mar	14000	3000	285.7	20
Apr	13000	3500	514.3	30
May	12500	4500	857.1	40
Jun	10000	5000	1142.9	60
Jul-Sep	Flow predominantly due to monsoon rain			
Oct	6000	1500	57.1	80
Nov	7000	500	14.3	80
Dec	10000	Nil	Nil	Nil

period. This statement is illustrated in Fig. 6 for the year 1986. The two curves intersect around third week of April. By this time, the contribution of snowmelt to river run-off increases significantly as a consequence of snow cover depletion. The position of the line PQ in the figure is an important input for the prediction of snowmelt hydrograph during pre-monsoon months.

(*vi*) This work is an exercise based on scanty data of 3 years observations. Snow cover observations during accumulation and melt period are not available by any other means as there are no observations or survey team taking snowline observations. As such no conclusion can be drawn from the study. However, it is felt that with more regular data, this type of studies will yield more fruitful results.

APPENDIX

Meteorological data recorded at Shimla used to estimate *Ta* & *Ts*

Date	Cloudiness (*N*) in decimal fraction	Wind speed (m/sec)	Max temp (°C)	Min temp (°C)	*Ta*	*Ts*
		1985				
18 Oct	0	1.73	17	7	4	0
23 Nov	0	1.15	12	5	—3	—2
02 Dec	0	0.58	13	5	—2	—1
10 Dec	0	1.73	10	3	—4	—3
19 Dec	0.25	0.58	10	2	4	0
		1986				
07 Jan	0.20	2.30	15	4	12	0
15 Jan	0	2.30	11	0	8	0
07 Feb	0	1.73	13	3	6	0
19 Feb	0.06	1.73	7	1	5	0
05 Mar	0	1.15	15	6	9	0
16 Mar	0.20	2.30	10	1	5	0
21 Apr	0.06	1.15	24	16	13	0
30 Apr	0	1.15	21	11	9	0
05 May	0	2.30	23	13	8	0
		1987				
08 Jan	—	0.58	11	5	9	0
04 Feb	—	1.73	11	0	3	0
07 Feb	0.06	1.73	14	4	5	0
20 Apr	0.31	0.58	23	15	12	0
27 May	0.06	0.58	25	15	10	0
06 Jun	—	0	27	18	7	0
13 Jun	—	0.58	25	15	4	0

References

Corps of Engineers, U.S. Army, 1956, Summary of Reports on Snow Hydrology.

Meir, M.J., 1975, Applications of Remote Sensing Techniques in Seasonal Snow Covers, *J. Glaciology*, **15**.

Rango, A. and Salomonson, V.V., 1976, Satellite snow observations and seasonal streamflow forecasts, Final Report, NOAA, Contract No. NA-776-74; NESDIS.

Schneider, S.R., Weisnet, D.R. and McMillin, M.C., 1976, River Basin Snow mapping at the National Environmental Satellite data and Information Service, U.S. Dept. of Commerce, USA.

Upadhyay, D.S., 1981, "A study on Heat Transfer in Seasonal Snow Cover" *Mausam*, **32**, 4, pp. 411-414.

Upadhyay, D.S , 1983, Thesis on Variation in specific properties of seasonal snow cover, Banaras Hindu University.